Electronic Supplementary Material (ESI) for RSC Advances.


# Insights in metal retention role on the antibacterial behavior of montmorillonite and cellulose supported copper and silver nanoparticles

Farzaneh Noori et al.

## SUPPORTING INFORMATION

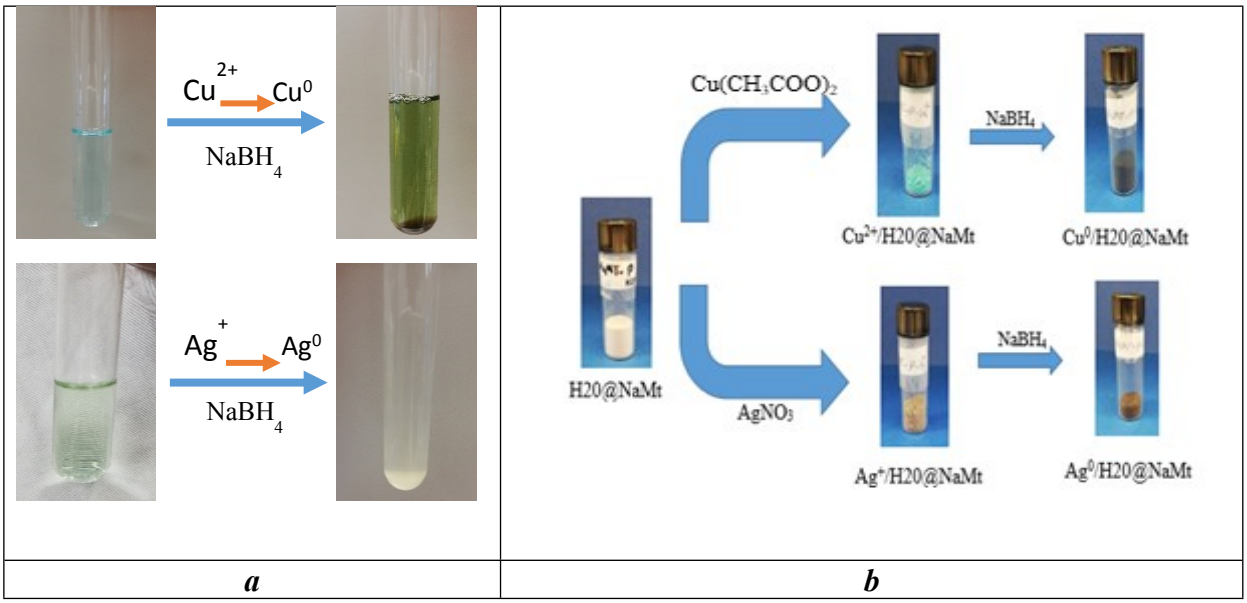


**Fig. S1.** Color changes after reduction of $Cu^{2+}$ and $Ag^{+}$ in the presence of $NaBH_4$ (a) and color changes of H20@NaMt composites after $MNP_S$ and cation incorporation (b).

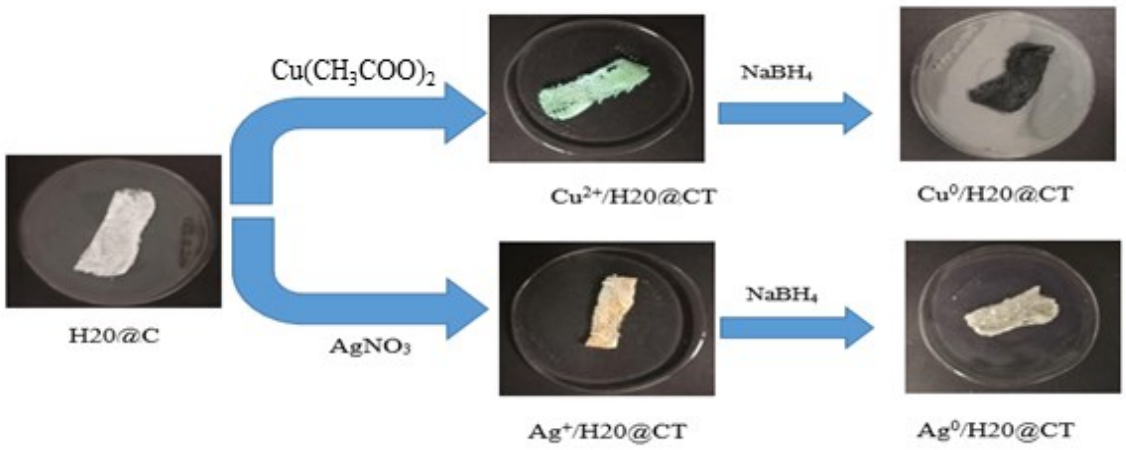


**Fig. S2**. Color changes of cellulose-based samples after the dispersion of metal cation and metal nanoparticles without or with the presence of $NaBH_4$ respectively.

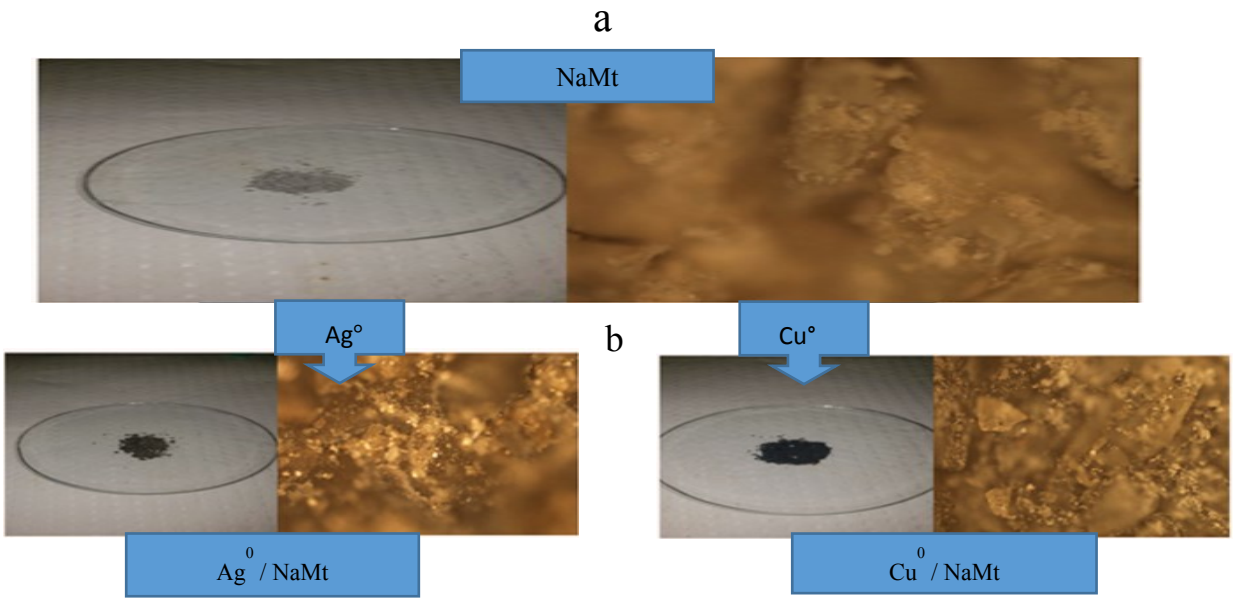


**Fig. S3.** Color changes and optical microscopy images of untreated NaMt (a) and MNPs-loaded NaMt (b).

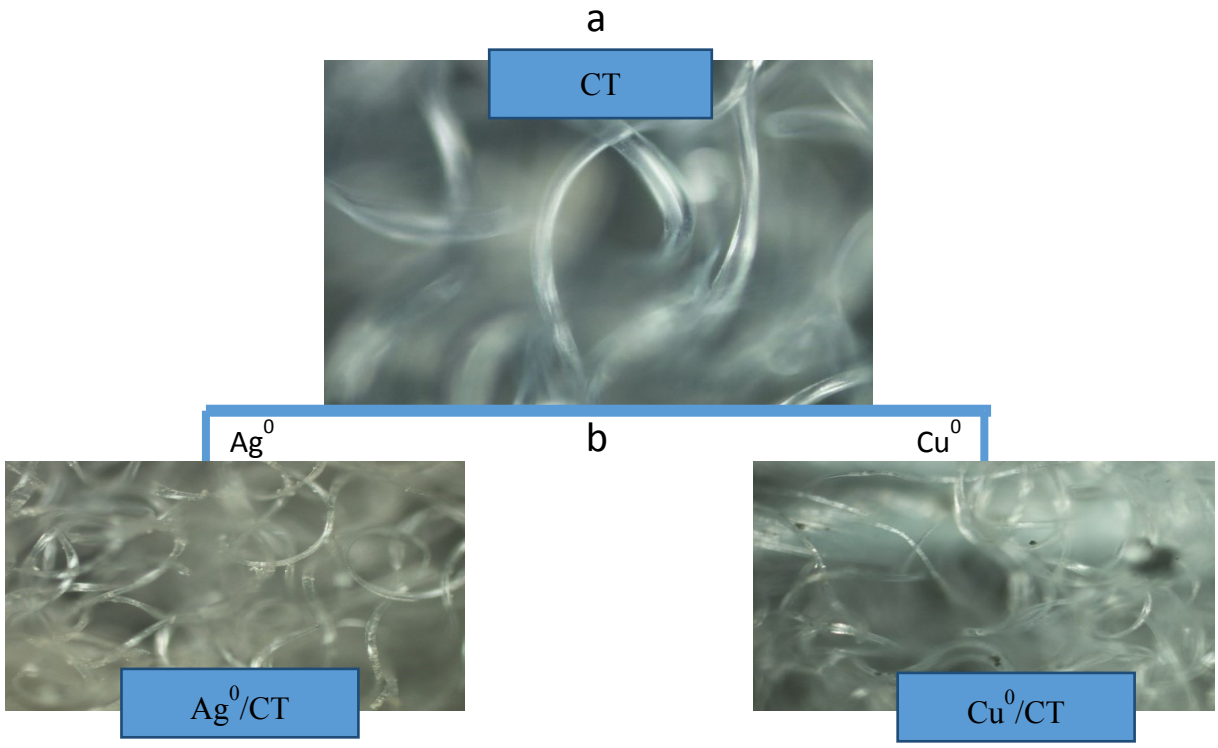


**Fig. S4.** Color changes and optical microscopy image of untreated CT (a) and MNPs-loaded CT (b).

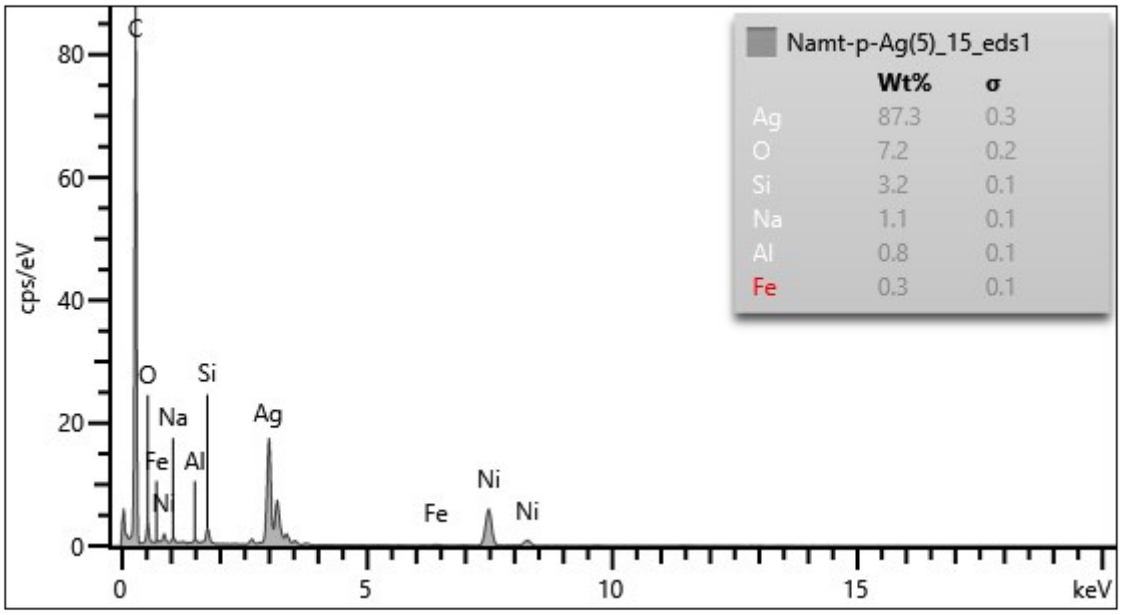
Namt-p-Ag(5)_15_eds1
Wt% σ
Ag 87.3 0.3
O 7.2 0.2
Si 3.2 0.1
Na 1.1 0.1
Al 0.8 0.1
Fe 0.3 0.1
cps/eV
keV
C
O
Si
Na
Ag
Fe
Al
Ni
Fe
Ni
Ni

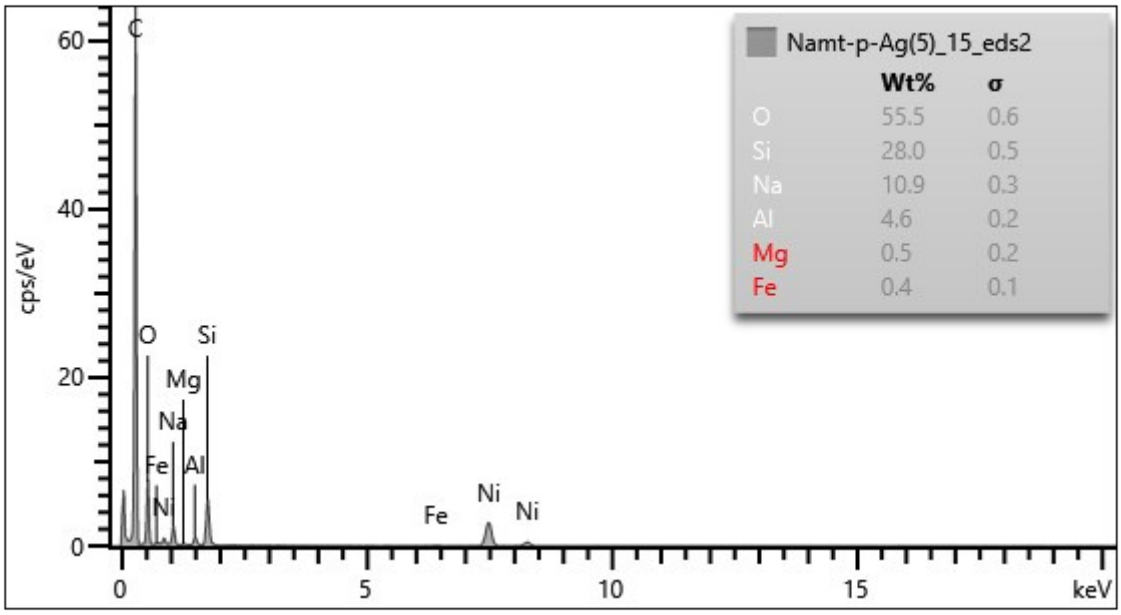
Namt-p-Ag(5)_15_eds2
Wt% σ
O 55.5 0.6
Si 28.0 0.5
Na 10.9 0.3
Al 4.6 0.2
Mg 0.5 0.2
Fe 0.4 0.1
cps/eV
keV
C
O
Si
Mg
Na
Fe
Al
Ni
Fe
Ni
Ni

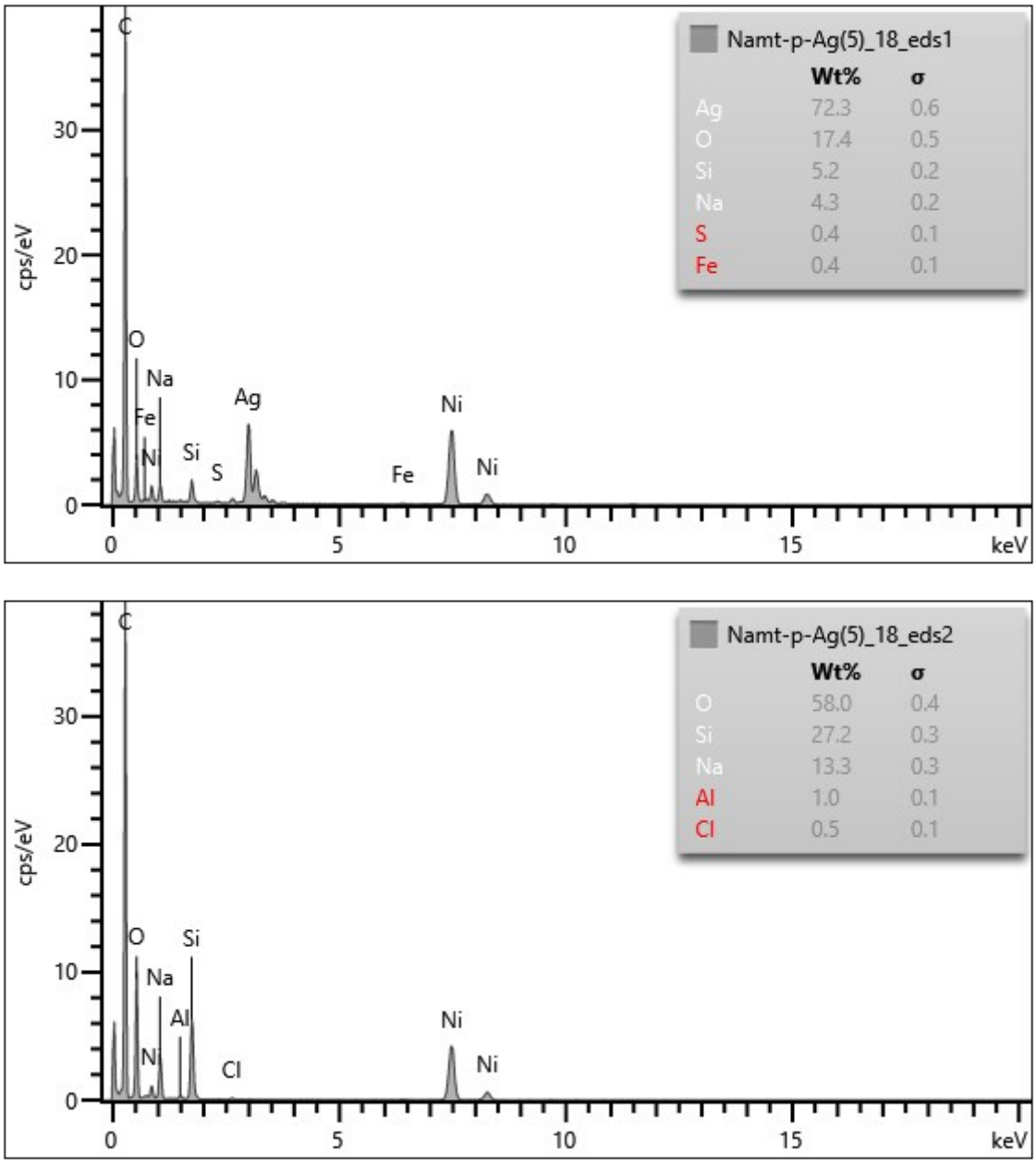


**Fig. S5.** ED-XRF spectra of some spots on SEM images of $Ag^0$/H20-NaMt.

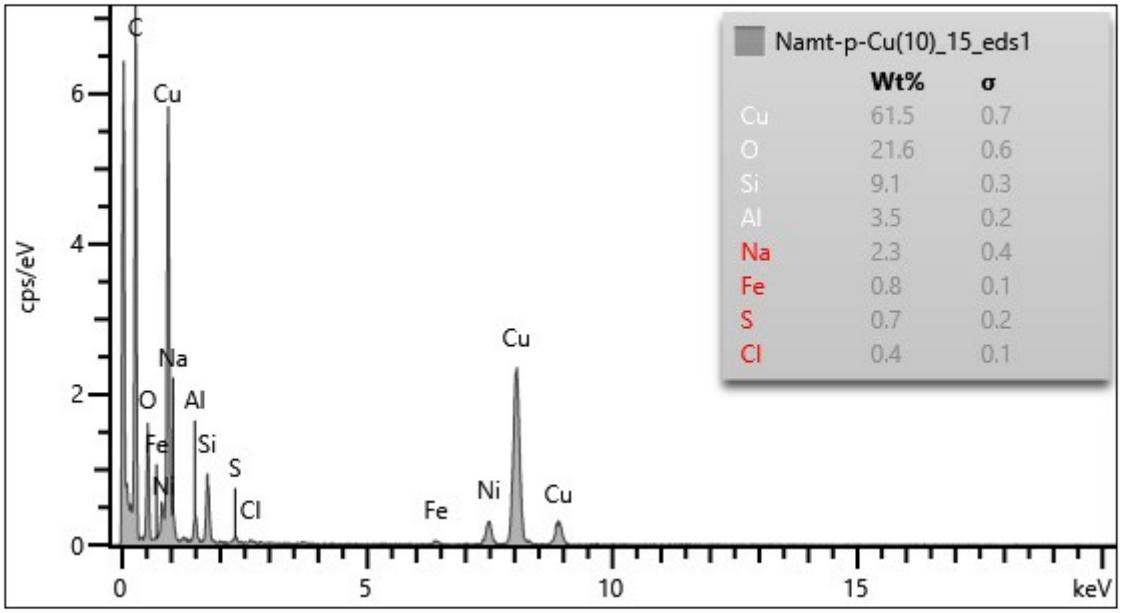
Namt-p-Cu(10)_15_eds1
Wt% σ
Cu 61.5 0.7
O 21.6 0.6
Si 9.1 0.3
Al 3.5 0.2
Na 2.3 0.4
Fe 0.8 0.1
S 0.7 0.2
Cl 0.4 0.1
cps/eV
keV
C
Cu
Na
O
Al
Fe
Si
S
N
Cl
Fe
Ni
Cu
Cu

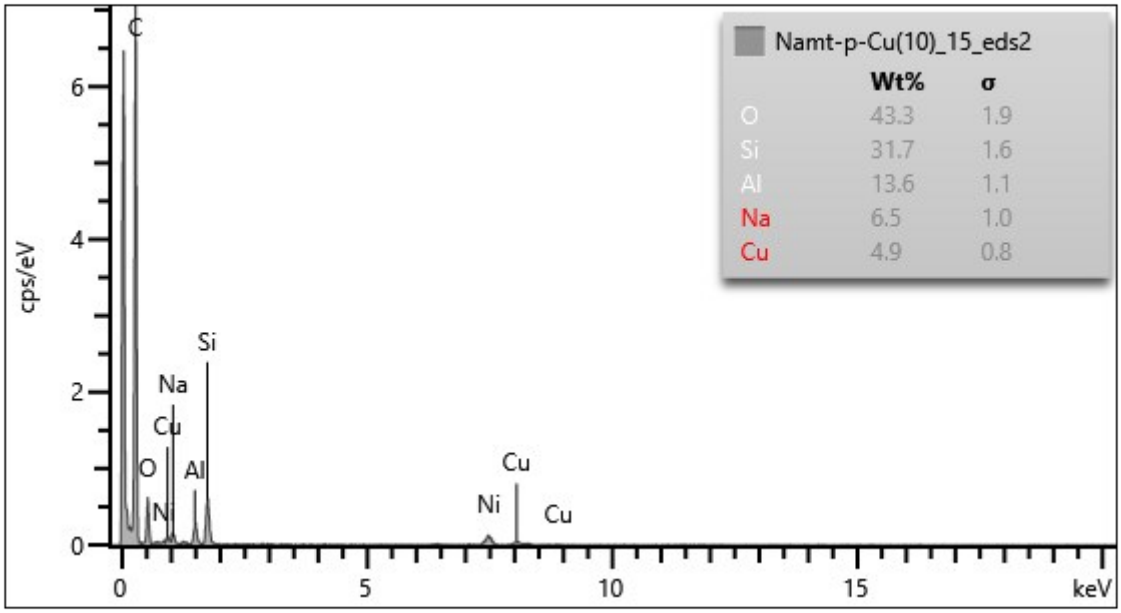
Namt-p-Cu(10)_15_eds2
Wt% σ
O 43.3 1.9
Si 31.7 1.6
Al 13.6 1.1
Na 6.5 1.0
Cu 4.9 0.8
cps/eV
keV
C
Si
Na
Cu
O
Al
N
Ni
Cu
Cu

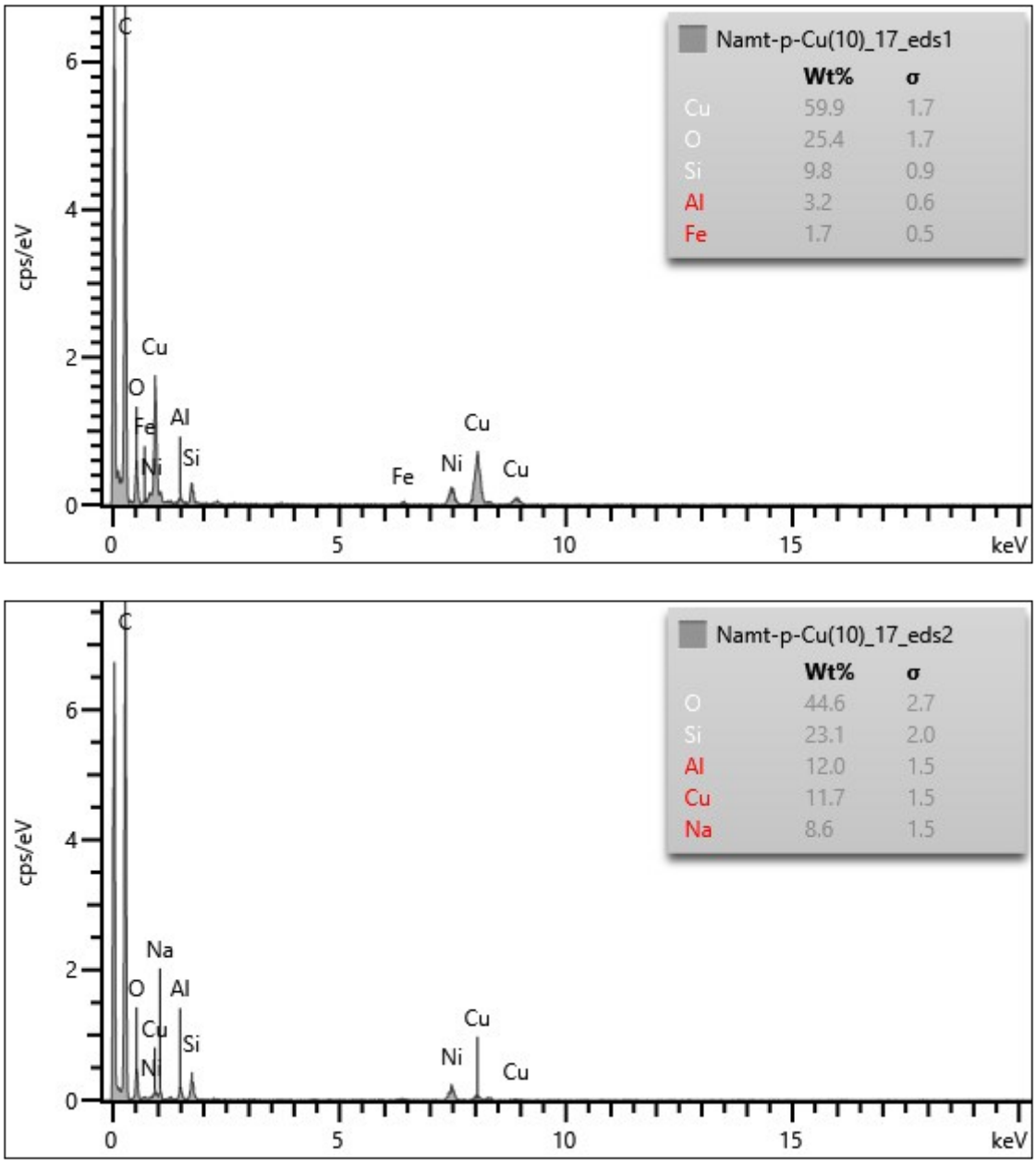


**Fig. S6.** ED-XRF spectra of some spots on SEM images of $Cu^0$/H20-NaMt.

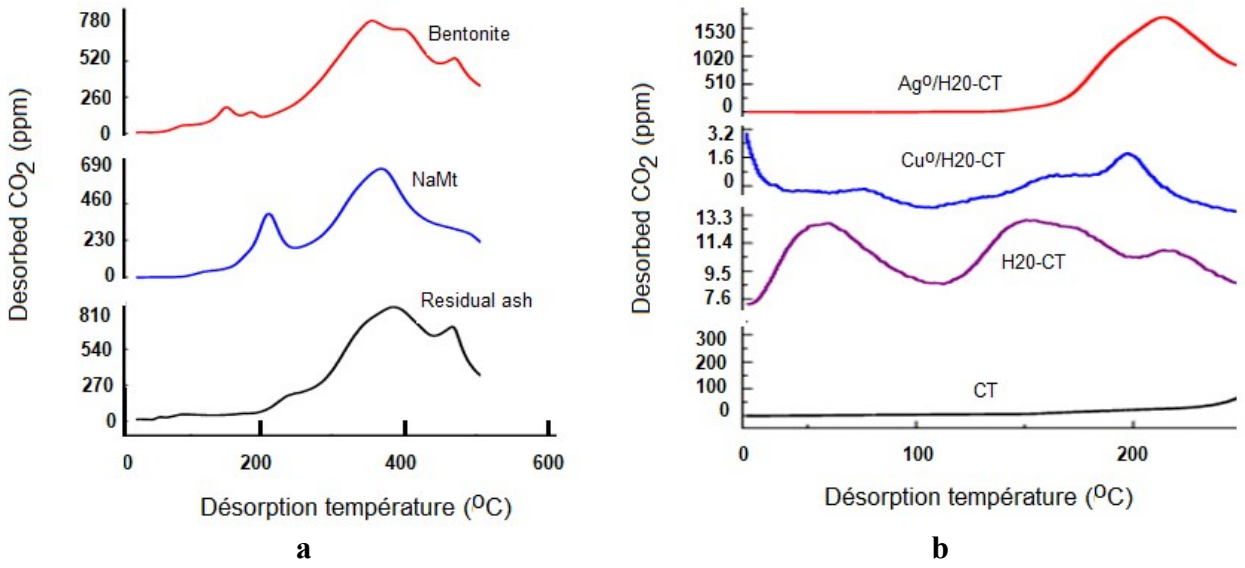


**Fig. S7.** $CO_2$-TPD patterns of clay-based samples (a) and CT-based samples (b):

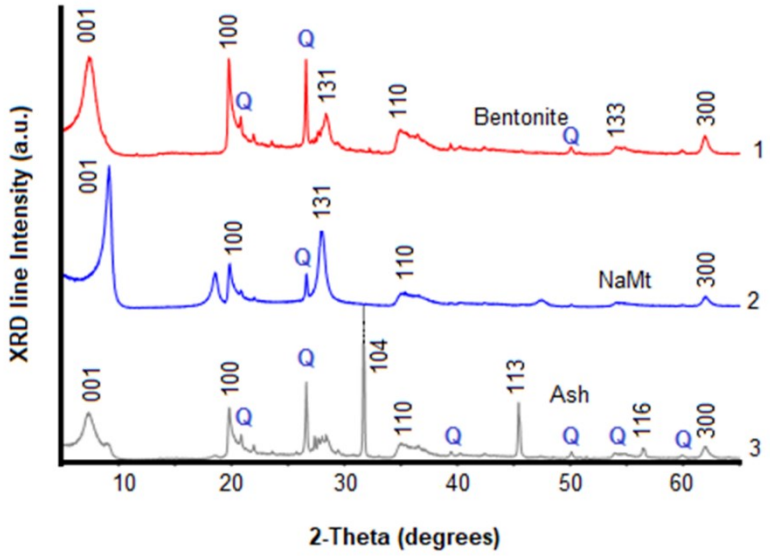


**Fig. S8.** XRD patterns of bentonite (1), NaMt (2)) and residual ash from bentonite purification (3).

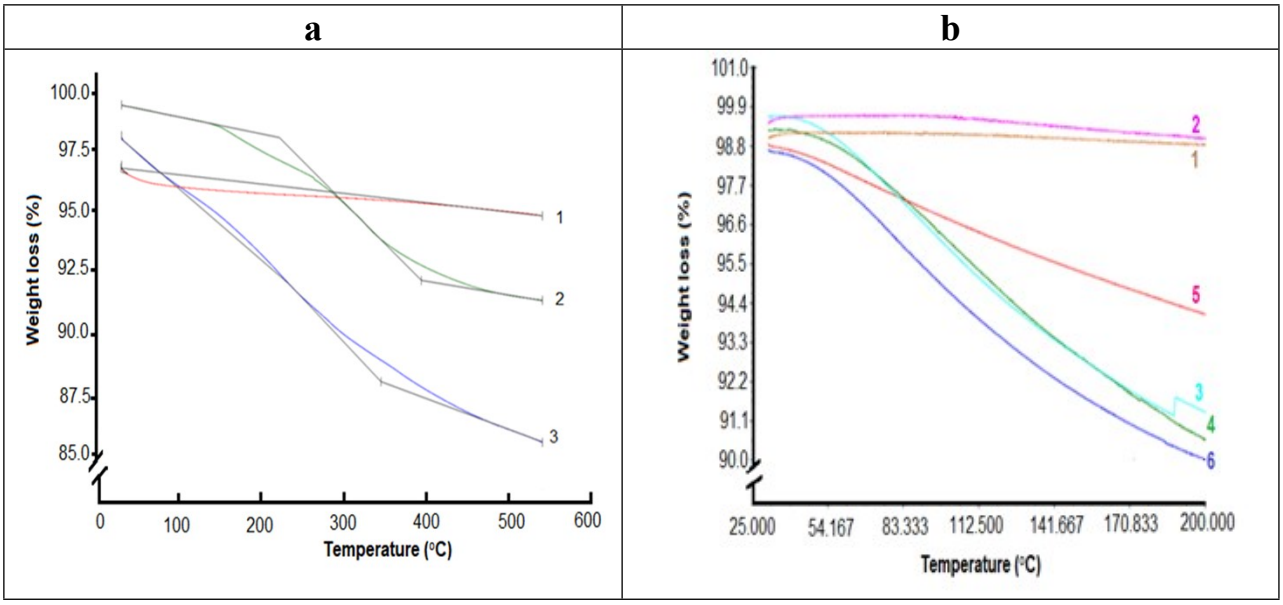


**Fig. S9.** TGA patterns of (a) clay-based samples: NaMt (1), $Cu^0$/NaMt (2) and $Ag^0$/NaMt (3) and of (b) Celluloase-based materials: CT (1), H20-CT (2), $Cu^0$/CT (3), $Ag^0$/CT (4), $Cu^0$/H20-CT (5) and $Ag^0$/H20-CT (6). TGA patterns were recorded between 25 and 700 °C for clay based samples and between 25 and 200 °C for CT-based materials.

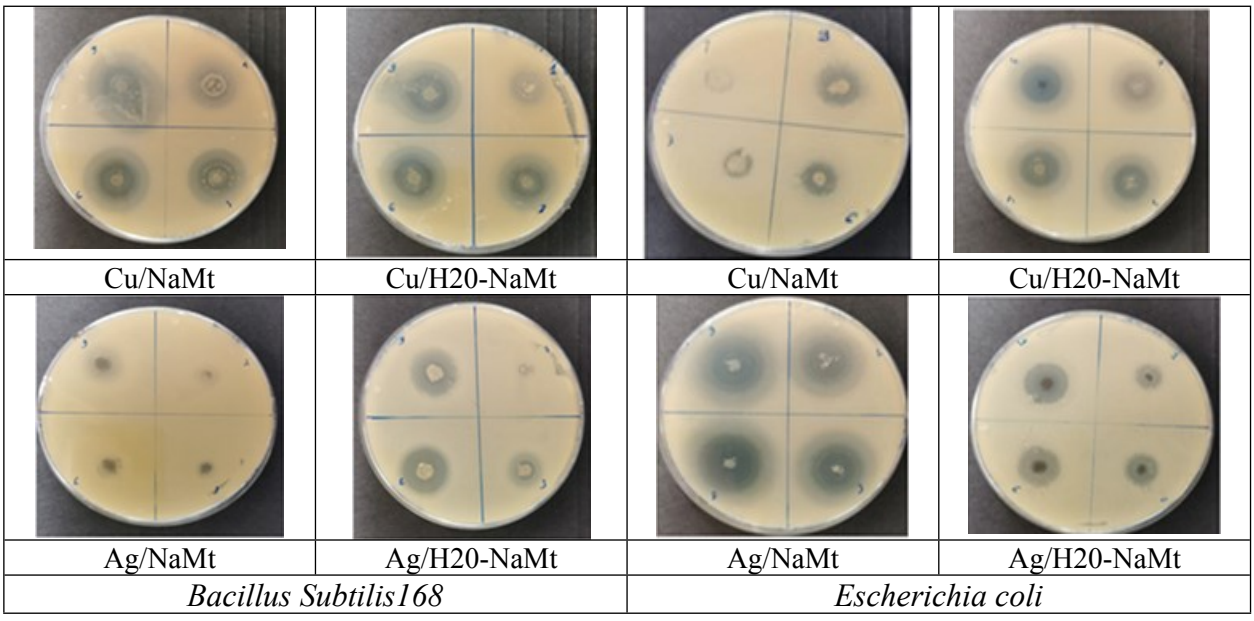


**Fig. S10.** Inhibition zones in *Bacillus Subtilis168* proliferation in the presence of NaMt (a) and metal-loaded H20/NaMt composites (b).

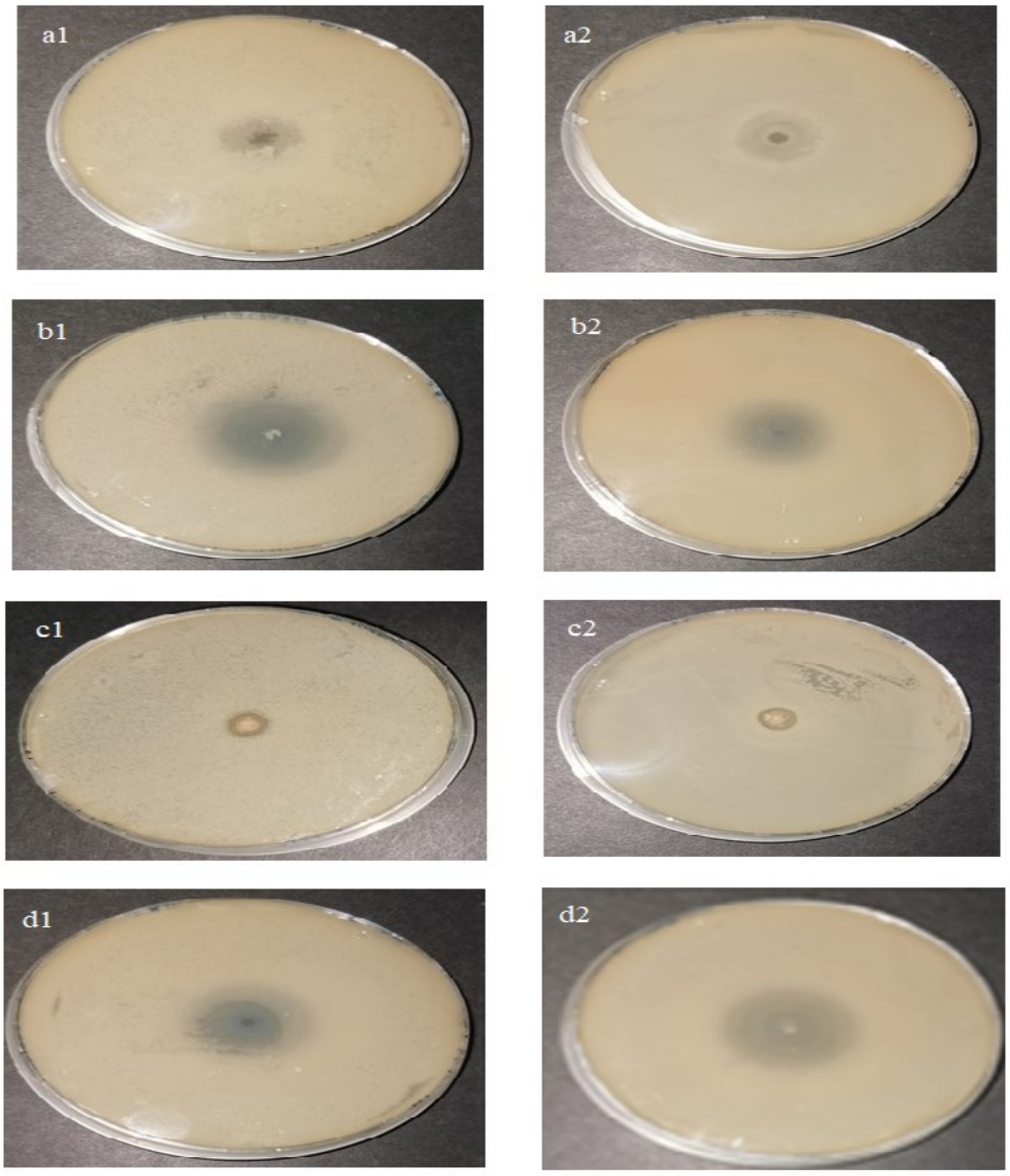


**Fig. S11. Antibacterial test of MNP loaded in organoclay- based samples**. *Escherichia coli* (a1, b1, c1 and d1), *Bacillus subtilis168* (a2, b2, c2 and d2) were incubated for 24h at 37 °C with 5 mg of $Ag^0$/H20@NaMt (a1-2); $Cu^0$/H20@NaMt (b1-2); $Ag^+$/H20@NaMt (c1-2) and $Cu^{2+}$/H20@NaMt (d1-2). **This figure should be redesigned as those made by me (Azzouz).**

**Table S1.** Zeta potential, particle size and inhibition zone diameter for clay-based samples

| Samples | Zeta potential (mV)* | Particle size (nm)** | pH | Inhibition zone diameter (cm) | |
|---|---|---|---|---|---|
| | | | | *E. coli* DH5α | *B. subtilis 168* |
| NaMt | -26.56 | 342.7 | 6.01 | 0 | 0 |
| Boltorn H20 | -28.57 | 201.2 | 4.62 | 0 | 0 |
| $Cu^0$/NaMt | -23.19 | 221.2 | 9.28 | 1.40 | 1.83 |
| $Ag^0$/NaMt | -28.31 | 152.7 | 9.08 | 1.87 | 1.83 |
| H20-NaMt | -38.12 | 373.7 | 7.59 | 0 | 0 |
| $Cu^0$/H20-NaMt | -26.91 | 164.2 | 9.25 | 1.77 | 1.83 |
| $Ag^0$/H20-NaMt | -27.21 | 127.6 | 9.16 | 1.07 | 1.50 |

*Average error on Zeta potential = 6.7%; **Average error on particle size = 5.7%.

**Table S2.** Inhibition zone diameters (cm) for different amounts of metal-loaded clay samples.

| Samples | *B. subtilis 168* | | | | *E. coli DH5α* | | | |
|---|---|---|---|---|---|---|---|---|
| Concentrations (mg powder) | 1 | 3 | 6 | 9 | 1 | 3 | 6 | 9 |
| NaMt-$Cu^0$ | 2,0 | 2,3 | 2,6 | 3,2 | 0 | 0,2 | 1,3 | 1,6 |
| NaMt-$Ag^0$ | 0 | 0 | 0,7 | 1,5 | 0 | 0,9 | 1,3 | 1,6 |
| $Cu^0$/NaMt@H20 | 1,3 | 1,3 | 1,7 | 3,0 | 0,6 | 1,7 | 2,1 | 2,4 |
| $Ag^0$/NaMt@H20 | 0,7 | 1,3 | 2,1 | 2,2 | 0,9 | 1,4 | 1,6 | 1,8 |
| $Cu^{2+}$/NaMt@H20 | 2,3 | 2,8 | 3,4 | 3,5 | 2,0 | 2,4 | 2,5 | 2,5 |
| $Ag^+$/NaMt@H20 | 2,0 | 2,8 | 3,3 | 3,3 | 0,8 | 1,1 | 1,2 | 1,7 |